Cochlear implants: Modeling electrophysiological responses

Gendt, M.J. van

CHAPTER 6

Simulating intracochlear electrocochleography with a combined model of acoustic hearing and electric current spread in the cochlea

Margriet J. van Gendt
Kanthaiah Koka
Randy K. Kalkman
H. Christiaan Stronks
Jeroen J. Briaire
Leonid Litvak
Johan H. M. Frijns

The Journal of the Acoustical Society of America 2020 (147), 2049

ABSTRACT

Intracochlear electrocochleography (ECochG) is a potential tool for the assessment of residual hearing in cochlear implant users during implantation and of acoustical tuning post-operatively. It is, however, unclear how these ECochG recordings from different locations in the cochlea depend on the stimulus parameters, cochlear morphology, implant design or hair cell degeneration. In this paper a model is presented that simulates intracochlear ECochG recordings by combining two existing models, namely a peripheral one that simulates hair cell activation, and a three-dimensional (3D) volume-conduction model of the current spread in the cochlea. The outcomes were compared to actual ECochG recordings from subjects with a cochlear implant (CI). The 3D volume conduction simulations showed that the intracochlear ECochG is a local measure of activation. Simulations showed that increasing stimulus frequency resulted in a basal shift of the peak cochlear microphonic (CM) amplitude. Increasing the stimulus level resulted in wider tuning curves as recorded along the array. Simulations with hair cell degeneration resulted in ECochG responses that resembled the recordings from the two subjects in terms of CM onset responses, higher harmonics and the width of the tuning curve. It was concluded that the model reproduced the patterns seen in intracochlear hair cell responses recorded from CI-subjects.

1 INTRODUCTION

Clinically, extracochlear electrocochleography (ECochG) is an established tool in the objective diagnosis of hearing loss, Meniere's disease and retro-cochlear pathologies (Davis et al., 1958; Ferraro et al., 1985; Gibson, 1983; Gibson et al., 1977; Morrison et al., 1976; Schoonhoven et al., 1996). In ECochG, electrical potentials generated by hair cell and neural activity in response to acoustic stimulation are recorded by an electrode, usually placed close to the round window. The ECochG response is recorded in response to both condensation and rarefaction stimuli, which are then subtracted to obtain the difference response or added to obtain the summed response. The difference response reveals the cochlear microphonic (CM). The CM is defined as the amplitude in the difference response at stimulus frequency. The difference response consists mostly of hair cell, but also some neural activity. The latter is referred to as the auditory nerve neurophonic (ANN) (Fontenot et al., 2017; Forgues et al., 2014; Tasaki et al., 1954). The summed response contains the summating potential (SP) originating from hair cell activity, and the compound action potential (CAP) and ANN originating from neural activity (Dallos, 1986, 1985, 1984; Davis et al., 1958; Durrant et al., 1998; Forgues et al., 2014; Russell and Sellick, 1977; Tasaki et al., 1954).

Nowadays, ECochG can readily be recorded intracochlearly through the use of the reverse telemetry functionality of cochlear implants. Intracochlear ECochG recordings are different from the widely described extracochlear ECochG recordings in the sense that they are recorded much closer to the source and can hence be higher in amplitude. Moreover, they can be recorded by electrodes along the length of the array. Intracochlear ECochG can be used to detect hair cell damage during cochlear implantation surgery (Calloway et al., 2014; Campbell et al., 2017; Choudhury et al., 2012; Harris et al., 2017; Helmstaedter et al., 2018; Koka et al., 2017b), allowing for direct feedback to the surgeon (Campbell et al., 2015; Dalbert et al., 2015; Koka et al., 2017b; Mandalà et al., 2012). Sudden drops in CM amplitudes are hypothesized to be related to hair cell damage during insertion (Giardina et al., 2019; Koka et al., 2018). Feedback of the CM amplitude is believed to lead to more controlled insertions, which can reduce the risk of cochlear damage. This risk is particularly relevant for patients with ski-slope hearing losses, which can be treated with electric and acoustic stimulation (EAS) (Gantz and Turner, 2010). EAS allows the high-pitched sound perception induced by electrical stimulation to be complemented with low acoustic frequencies delivered by a hearing aid.

Intracochlear ECochG can also be used postoperatively, to measure residual hearing objectively. This procedure is particularly relevant for recipients where acoustic thresholds are difficult to obtain subjectively (e.g., young children). Intracochlearly recorded CM amplitudes were shown to correlate to the frequency-specific audiometric thresholds (Koka et al., 2017b, 2017a). Additionally, the acoustic tuning of the electrodes can be determined postoperatively, allowing for the matching of acoustic and electrical frequencies in the EAS system (Campbell et al., 2017).

The number of studies reporting recordings of intracochlear ECochG responses from CI-subjects during surgery (Calloway et al., 2014; Dalbert et al., 2015; Giardina et al., 2019; Harris et al., 2017; Koka et al., 2018) or post-operatively (Tejani et al., 2019) is increasing. However, at present, it is unknown how the response depends on exact intracochlear recording position and how it is affected by stimulus- and patient-specific factors. Such knowledge is vital for the interpretation of intracochlear ECochG recordings during insertion or post-operatively along the array.

The potentials arising in the cochlea in response to sound depend on stimulus characteristics and cochlear health (Dallos and Cheatham, 1976; Davis et al., 1958). Sensitivity of the recording electrodes at different positions in the cochlea to these potentials depends on the distance, cochlear morphology, electrode design and electrical properties of the cochlear tissue. The exact location of the implanted electrode, and related the distance from current sources such as hair cells to the implanted electrode, depends on cochlear morphology and electrode design(van der Jagt et al., 2017). Electrical properties of the tissue also affect the sensitivity of the electrode to the different current sources. Previously, modeling studies have been used to estimate the electrical attenuation along the basilar membrane. However, these studies have yielded incongruent estimates, with reported values ranging from 2 to 30 dB/mm (Ayat et al., 2015; Charaziak et al., 2017; Davis et al., 1958; Dong and Olson, 2013; Fridberger et al., 2004; Mistrík et al., 2009; Tasaki and Fernández, 1952; Teal and Ni, 2016; v. Békésy, 1952, 1951; Whitfield and Ross, 1965).

A detailed 3D model of the cochlea, that is verified for its simulations of electrical conductivities for the implanted electrode, could provide accurate simulations. The combination of the electrical potentials arising in the cochlea in response to sound stimulus and how they are conducted in the cochlea determine the ECochG response at each different location.

The goal of the current study was to aid in the interpretation of intra- and postoperative ECochG recordings, by modeling these responses. In such a model, both the potentials arising in the cochlea in response to sound and the attenuation of potentials within the cochlea must be included. To accomplish this, a model of the auditory periphery predicting hair cell responses was combined with a 3D model of current spread. Effects of stimulus frequency and level, recording electrode, cochlear morphology, electrode design and hair cell damage were tested. The model was compared to intracochlear ECochG recordings from two CI-subjects.

2 METHODS

Intracochlear ECochG hair cell responses were simulated with a combined model of inner hair cell (IHC) and outer hair cell (OHC) activation throughout the cochlea (Zilany et al., 2014; Zilany and Bruce, 2006) and of current spread in the cochlea (Kalkman et al., 2015, 2014). The following sections describe the model. Section A describes how hair cell potentials are simulated. Section B describes how electrical attenuation, for different cochlear morphologies and electrode designs, is modeled. Section C describes how both models were combined to calculate the intracochlear ECochG response. Hearing loss was modeled by including different types of hair cell degeneration, the approach hereto is described in section D. Lastly, section E describes how subject recordings were performed.

2.1 Modeled hair cell responses

The voltages over the IHC and OHC membranes were calculated with a model of the auditory periphery developed by Zilany et al. (Bruce et al., 2018, 2003; Carney, 1993; Zhang et al., 2001; Zilany and Bruce, 2006). The model is freely available on the internet. A schematic diagram of the model is shown in Figure 6.1.

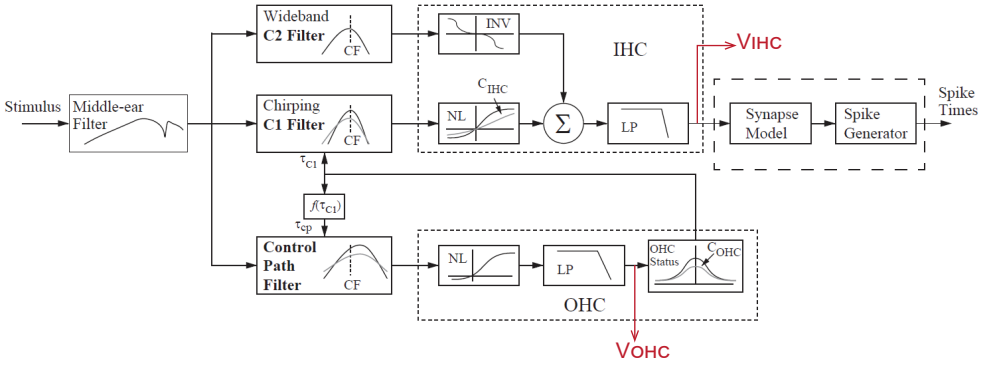

Figure 6.1. Schematic diagram of the auditory-periphery model used to calculate the intracellular voltages. The stimulus is the sound pressure waveform in Pa and the outputs used in the current paper are the intracellular voltages VIHC and the VOHC for the inner hair cell (IHC) and outer hair cell (OHC) respectively. These potentials are extracted immediately after the Non-Linearity (NL) and the Low-Pass Filter (LP), as indicated by the red arrows. The model includes a middle-ear filter, inner hair cell (C1 and C2) and outer hair cell (control) pathways, a synapse and spiking model. COHC and CIHC are scaling constants that control OHC and IHC status. CF: characteristic frequency, INV: inverting nonlinearity. [from Zilany and Bruce, 2006, reprinted with permission]

The auditory periphery model included a middle ear filter, inner hair cell and outer hair cell pathways, a synapse model and a spike generator. Human cochlear tuning was used (Shera et al., 2002). Each hair cell had a scaling constant ('C-factor') that described its physiological health. The C-factor could be adjusted from 1 for healthy hair cells, to 0 for complete functional loss for IHCs and OHCs separately. The C_{OHC} had an effect on the bandwidth of the

inner hair cell pathway. The potentials over the hair cell membranes were extracted at the output of the cochlear pathways. This auditory peripheral model was previously validated by comparing spiking behavior in auditory nerve (AN) fibers generated by the model to physiological data from single fiber and membrane voltage recordings in cats (Bruce, 1997; Bruce et al., 2018; Zhang et al., 2001; Zilany et al., 2014, 2009; Zilany and Bruce, 2006). It was shown that level- and frequency-dependency of auditory nerve fiber responses were correctly simulated by the peripheral model.

There were two modifications included in the analysis of the hair cell output for the current implementation; 1) scaling of outer hair cell contributions and 2) converting from membrane voltages to extracellular currents. The OHC voltages in the auditory peripheral model were originally applied only as a qualitative measure. For the current study, however, both inner and outer hair cell responses were needed. In animal recordings the responses of IHCs to stimulation with a tone of 800 Hz and 15 dB were four times larger than the responses of OHCs (Dallos, 1986, 1985). In the current study, the simulated OHC responses were scaled, such that the IHC Alternating Current (IHC-AC) response was four times larger than the IHC-AC response to acoustic stimulation at 800 Hz and 15 dB. OHC responses at other CFs, and in response to other stimulus frequencies, were scaled with the same factor. Comparison of the scaled simulations to previously published recordings from animal data (Dallos, 1986, 1985) (appendix A) showed that relative dependency of IHC and OHC intracellular hair cell potentials on stimulus level and frequency was qualitatively described by the model.

The original hair cell model simulates potential differences across the hair cell membranes. However, to model the ECochG, extracellular currents corresponding to these hair cell voltages were needed, which depend on the capacitive and conductive behavior of the hair cell membranes. Resistances across the apical membrane of the hair cell are modulated by the opening and closing of voltage-gated channels (Housley G.D. and Ashmore, 1992; Mammano and Ashmore, 1996). These resistances depend on the voltage over the membrane. The voltage-dependent conductance (G) can be fitted with the Boltzmann equation (Johnson et al., 2011):

$$G(V) = \frac{G_{max}}{1+e^{-(V-V_{0.5})/V_S}} \qquad \text{(Eq. 6.1)}$$

where $V_{0.5}$ is the voltage at the 50% point on the Boltzmann curve; G_{max} the maximum conductance; and V_S is the slope at the 50% point on the Boltzmann curve. For IHCs, the G_{max} = 470 nS, $V_{0.5}$ = −31 mV, V_S = 10 mV, and a resting potential V_{rest} of −55 mV. For OHCs, the $V_{0.5}$ equals −60 mV and is independent of characteristic frequency (CF). All other parameters depend on the CF. A linear fit performed on the data presented by Johnson et al. (2011) yielded: $Gmax(CF) = 0.02 \times CF + 40$, and $V_s(CF) = 8\ \exp^{-4} \times CF + 8.5$. The same paper showed that the hair cell membrane capacitance induced first-order low-pass filtering, with an IHC time constant $\tau = 0.26$ mV ($F_0 = 610$ Hz). For OHCs, the cut-off frequencies were shown to be higher than estimated previously, and increased linearly with the cells' CF, with a slope of nearly 1; the F_0 = CF and $\tau = 1/2\pi F_0$.

2.2 Volume conduction model

Intracochlear potentials resulting from hair cell currents were calculated using a volume conduction model of the implanted human cochlea (Kalkman et al., 2015, 2014). This volume conduction model, which uses the Boundary Element Method, was previously validated by comparison to clinically recorded intracochlear impedances (Kalkman et al., 2015, 2014). In the current study, electrical impedances from currents induced by hair cell activation to electrodes at different cochlear positions were calculated.

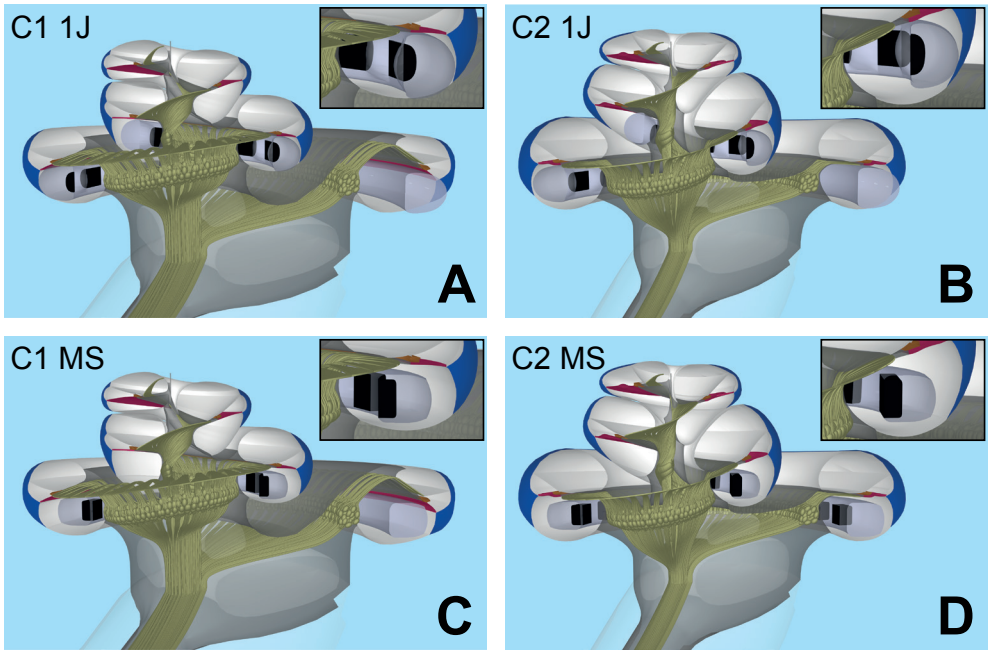

Figure 6.2. Cochlear morphologies C1 and C2 based on human histological sections implanted with 1J (straight, lateral wall) or MS (pre-curved, mid-scalar) electrodes in the scala tympani, which are plotted in grey with black electrode contacts. [A]: cochlea 1, electrode 1J; [B]: cochlea 2, electrode 1J; [C]: cochlea 1, electrode MS; [D]: cochlea 2, electrode MS.

To infer to which extent cochlear morphology and electrode placement caused inter-patient variability, two different cochlear morphologies and electrodes were implemented, figure 6.2. The cochlear morphologies and cross-sectional hair cell positions were based on individual histological sections of human cochleae, and differ for instance in their relative height and shapes of the different scalae. Two different electrode array designs were used for the simulations: a lateral wall, straight, HiFocus1J (Advanced Bionics) electrode (figure 6.2), and a pre-curved, HiFocusMS (Advanced Bionics) electrode, located in a mid-scalar position. The HiFocusMS electrode contacts were placed approximately equidistant from the basilar membrane, whereas the 1J electrode contacts were placed closer to the basilar membrane on the apical end and further from the membrane on the basal end.

3200 sets of hair cells were evenly distributed along the length of the basilar membrane, one row of IHCs and three rows of OHCs. Among these locations, 2840 sets of hair cells had CFs above 125 Hz. For those hair cells the auditory peripheral model could simulate voltage responses. Hair cells were considered dipoles, because of their anisotropic morphology and properties, and in line with a previous modeling study (Teal and Ni, 2016). The bottom pole of the current source of each hair cell was located in the basilar membrane, and the top pole of the current source was located in the scala media, as shown schematically in figure 6.3. The lengths of the dipoles varied throughout the geometries ranging from roughly 30 µm at the base of the cochlea to 70 µm at the apex (Pujol et al., 1992). In the cochlear geometries, the CF at a given position along the cochlea was determined by the Greenwood map (Kalkman et al., 2014). Simulated electrical potentials generated by the inner and outer hair cell dipoles and measured at the modeled recording contacts were divided by the dipole current amplitudes to obtain electrical impedance values for each dipole-contact pair.

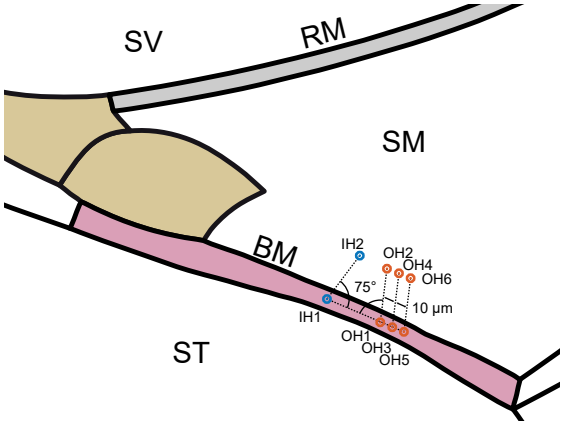

Figure 6.3. Mid-modiolar cross-section of the cochlea, centered around the scala media (SM), showing the hair cell positions of the three different rows of hair cells. SM = Scala Media, ST = Scala Tympani, SV = Scala Vestibuli, BM = Basilar membrane, RM = Reissner's membrane, IH1 = inner hair cell bottom, IH2, inner hair cell top, OH1, 3, 5 = outer hair cell bottoms in three different rows and OH 2, 4, 6 = outer hair cell tops in three different rows. A line drawn through the current dipoles was situated at an angle of 75° relative to the basilar membrane, with the IHCs and OHCs leaning towards each other. The three OHC dipoles were exactly parallel to each other and were positioned 10 µm apart, in the lateral direction along the basilar membrane.

The distances between individual dipoles were much smaller than the dimensions of the model's surface elements; therefore, some discretization/interpolation artifacts were present in the simulated electrical potentials. These artifacts were smoothed by applying a

spatial low-pass Butterworth filter to the potentials along the basilar membrane, induced by each row of 3200 dipoles.

2.3 Simulating intracochlear hair cell ECochG responses

The ECochG response for a recording electrode, *e*, was calculated as follows;

$$\mathrm{ECochG} = \sum_{hc=1}^{hc=last} Z_{VC}(hc, e) \cdot I_{hc} \qquad \text{(Eq. 6.2)}$$

Where I_{hc}, refers to all hair cell (hc) contributions, $Z_{VC}(hc, e)$ to the electrical impedance froe hair cell to the recording electrode as calculated by the Volume Conduction (VC) model (Kalkman et al., 2015, 2014). For each stimulus, the total ECochG response is calculated as the sum of contributions from all hair cells in time. Simulated sound stimuli were tone bursts with frequencies of 250, 500, 1000, 1500, 2000 and 4000 Hz with stimulus levels of 20- to 110-dB sound pressure level (SPL) with increments of 10 dB. The tone bursts had stimulus durations of 50 ms and rise and fall times of 0.5 ms. For all simulations, the sampling frequency was 100 kHz. The summation and difference response were obtained from the simulations of responses to condensation and rarefaction stimuli. The CM amplitude was calculated as the amplitude at the stimulus frequency in the difference response, obtained from the Fourier transform, over the response between 25 and 50 ms, to remove the onset response from this analysis.

2.4 Modeling hearing loss

Sensorineural hearing loss was simulated by lowering the number of surviving hair cells and by decreasing the C-factor. Six hypothetical types and degrees of hair cell degeneration were tested, namely:

- Only IHCs) All C-factors to 1, only responses from IHCs are considered
- Only OHCs) All C-factors to 1, only responses from OHCs are considered
- Hearing Loss (HL)-A) Equally distributed hair cell degeneration: hair cell survival 10%, C-factor of 1;
- HL-B) Equally distributed hair cell degeneration: hair cell survival 10%, C-factor of 0.1;
- HL-C) Sloping hair cell degeneration: hair cell degeneration decreased with CF from 100% apically to 0% in the base. The C-factor was related to the hair cell degeneration. This resulted in 100% survival in the apex combined with a c factor of 1, 50% survival and C-factor of 0.5 in the middle, and 0% survival and C-factor of 0 in the base;
- HL-D) Dead basal region: No hair cell degeneration in the basal 1/3rd of the cochlea, and 10% survival elsewhere combined with a C-factor, of 0.1.

An overview of the parameters in the six types and degrees of hair cell degeneration is given in table 6.1.

Table 6.1. Overview of parameters in the six different hair cell degeneration

HL	Shape	Survival rate	c-factor
ihc	Flat	100%	1
ohc	Flat	100%	1
A	Flat	10%	1
B	Flat	10%	0.1
C	Sloping	100% apical to 0% basal	1 apical to 0 basal
D	Dead region	10% apical and mid, 0% basal	0.1 apical and mid, 0 basal

2.5 Subject recordings

Intracochlear ECochG responses were recorded in two subjects with CIs with residual hearing in the implanted ear. Data on the hearing loss and implants of these subjects is given in table 6.2.

Table 6.2. Audiograms and subject information for the two subjects (ID-1 and ID-2). Audiogram values are the thresholds (dB_{HL}) at each frequency

Pt	Audiogram Frequency, Hz					Subject information				
	125	250	500	1000	2000	CI use	Ear	Age	Cause	Device
ID-1	25	40	50	55	50	3 yrs	R	57	SNHL	Advantage, HiFocus MS
ID-2	55	60	70	75	>100	3 yrs	R	85	SNHL	Advantage, HiFocus MS

Acoustic stimulations were done with 50 ms tone bursts, with 1 cycle each for the ramp up and the ramp down, with a Hanning window. In the recordings a bin-width of 36 Hz was achieved with a rate of 9280 Hz and 512 samples. The signal was defined as the amplitude of the Fourier transform at the stimulus frequency. The initial stimulus amplitude was 110 dB SPL and was decreased in 10-dB steps until the signal-to-noise ratio was below 18 dB. Noise amplitude was defined as the average amplitudes of 4 to 6 bins flanking the stimulus frequency. Alternatively, in the absence of a distinct peak at the stimulus frequency, up to 40 averages were registered.

3 RESULTS

Simulated attenuation of currents within the cochlea, or modeled current distributions, are shown in section A. Section B reports on recordings and simulations of intracochlear ECochG potentials, both in the time- and frequency- domains. Section C investigates how the CM amplitude in response to different stimulus frequencies and amplitudes changes with exact recording position, and how it is affected by cochlear morphology, electrode design and hearing loss.

3.1 Electrical attenuation simulated by the volume conduction model

The simulated inner hair cell impedance curves are plotted in figure 6.4 for different cochlea-implant configurations.

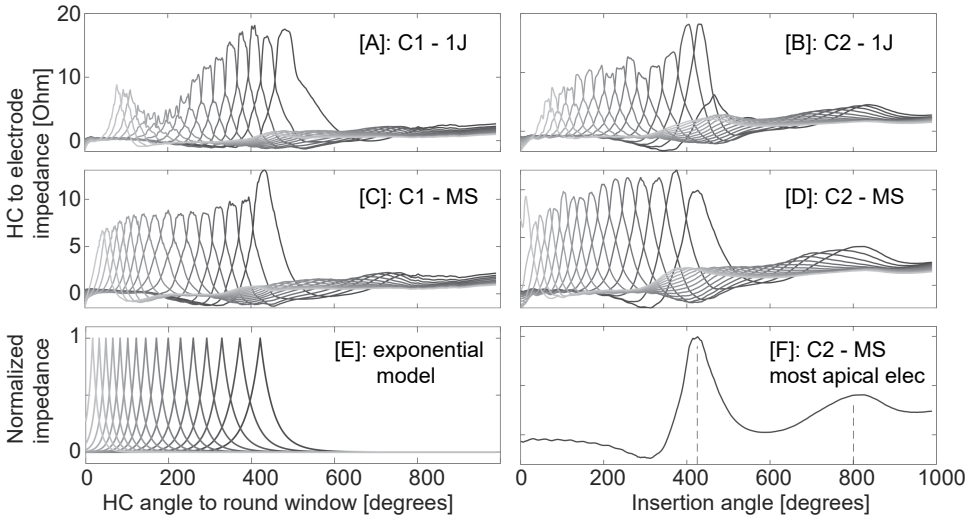

Figure 6.4. Electrode impedances in response to inner hair cell activities, modeled at 3200 different locations and 16 different electrode positions. Calculations were performed for the following configurations; [A] cochlea 1 - 1J; [B] cochlea 2 - 1J; [C] cochlea 1 - MS; [D] cochlea 2 -MS; [E] Exponential model; [F] impedance function for the most apical electrode contact from cochlea 2 - MS. Dotted lines in F indicate the sensitivity-peaks. Each curve corresponds to impedance values from all individual inner hair cells, measured at specific recording contact; hair cell locations are indicated along the x-axes as a function of insertion angle, measured from the round window.

Impedances between electrodes were more consistent in the MS array than in the 1J electrode. In the latter, impedances varied by as much as a factor of 3 between the least and most responsive electrode. In C2 the electrode contacts showed a moderately larger impedance to hair cells in the basal region. Figure 6.4F clearly demonstrates the double

peak in sensitivity to hair cell activation, in the exemplary impedance function for the most apical electrode in the C2-MS configuration. The regions of the peaks are almost 400 degrees apart, i.e., close to a complete turn (dotted lines), indicating cross-turn sensitivity.

3.2 Single electrode ECochG responses

This section describes ECochG responses simulated and recorded at the most apical electrode contact.

Single electrode recordings

ECochG summed and difference responses from two different subjects are shown in Figure 6.5. A temporal onset response was seen in the difference recording in subject ID-2, but not in the recording from subject ID-1. Higher odd harmonics in the spectral domain were also only seen in recordings from subject ID-2. In the summed responses recordings from subject ID-2 showed the first harmonic, whereas in subject ID-1 the even harmonics did not exceed the noise floor. There was no large direct current component in the recordings, probably due to high-pass-filtering of the recording set-up.

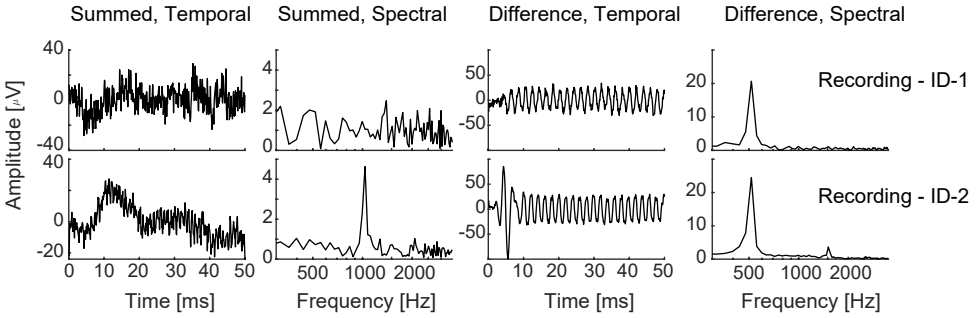

Figure 6.5. recorded ECochG responses to a 50-ms, 500-Hz, 100-dB SPL tone burst from subjects ID-1 and ID-2. The recordings were obtained from the most apical electrode contact.

Effect of hair cell damage on single electrode simulations

Figure 6.6 shows modeled ECochG summed and difference responses for different hair cell configurations. The amplitude of the AC component in the summed response varied among the different configurations of hair cell degeneration. The largest amplitude was seen in the healthy cochlea, and the smallest in hearing loss configuration B. The onset in the difference responses as observed in the recording of subject ID-2 was seen in some of the simulations; with the complete cochlea, with HL-A and with HL-C. The configurations used in these three simulations all included healthy inner and outer hair cells (in which C_{OHC} equals 1). The second harmonic was visible in almost all simulations, except for the simulation with only IHCs surviving, and was largest in again the complete cochlea, HL-A and HL-C. Difference responses from the simulations with only IHCs and only OHCs had nearly opposing phases, and the corresponding CM amplitudes were larger than from the

intact, complete cochlea. With any of the four HL simulations, amplitudes were around five times smaller than when all hair cells survived. Comparison to the subject recordings show that subject ID-1 best resembled the simulations without OHCs or HL-B or HL-D, since in these simulations no onset response was seen and higher harmonics were absent or small. Recordings from subject ID-2 closely matched the simulations with the complete cochlea, HL-A and HL-C, as these all showed a strong onset and higher harmonics.

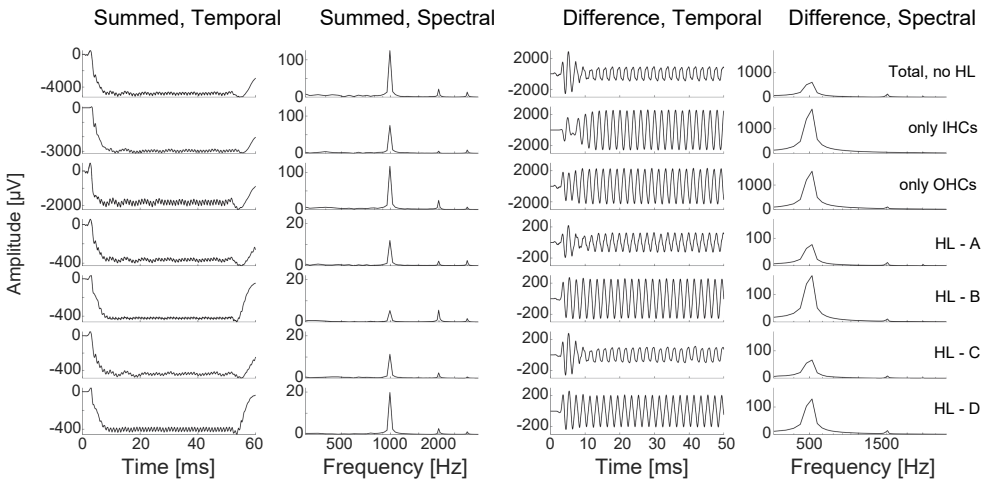

Figure 6.6. Simulated summed and difference responses for different hair cell configurations in both the temporal and the frequency domain. The top three rows show the responses from a cochlea when all hair cells, only the IHCs, or only the OHCs are taken into account, respectively. The other rows show responses for modeled hearing loss, namely 10% survival, c=1 (HL-A); 10% survival, c=0.1 (HL-B); sloping survival, sloping c (HL-C); no basal hair cells, other regions 10% survival and c=0.1 (HL-D).

3.3 CM along the array

This section explores the effects of stimulus configurations, cochlear morphology and electrode design, and hair cell survival on the CM amplitudes along the implanted array.

Effect of stimulus configuration

Figure 6.7 shows the recorded (two top rows) and simulated (two bottom rows) CM responses. The two bottom rows show CM simulations from the intact C1 cochlea with an MS array, stimulated with low (20 to 60 dB) and high (70 to 100 dB) stimulus levels respectively.

In both subjects as well as in the simulations, the response amplitudes increased as the stimulus intensity increased, and the peak-response shifted basally as the stimulus frequency increased. Subject ID-1 showed a narrow tuning. In subject ID-2, a second peak

appeared basally at most stimulus frequencies, when stimulated with 100- or 110-dB SPL. Simulated responses to low stimulus levels (figure 6.7, third row) showed narrow tuning, similar to the recordings from subject ID-1 (figure 6.7, first row). In response to higher stimulus levels, the simulated response amplitudes increased and the response became wider (figure 6.7, fourth row), which more closely resembled recordings from subject ID-2 (figure 6.7, second row).

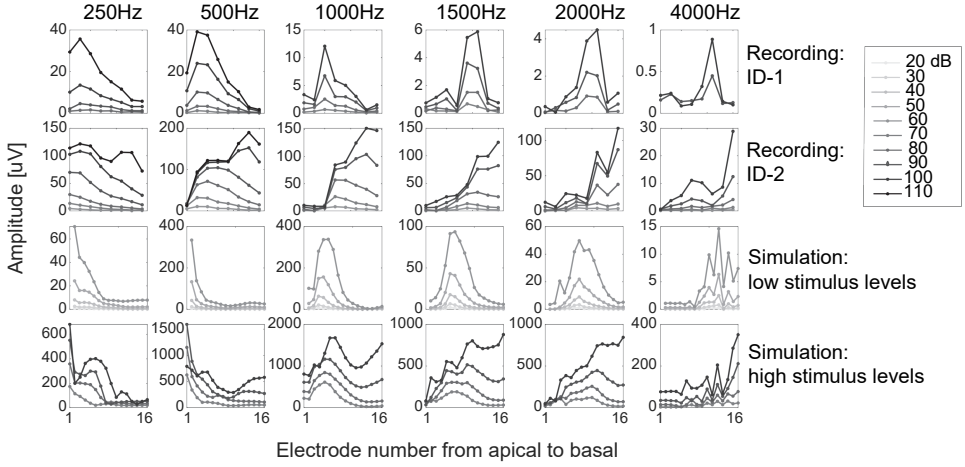

Figure 6.7. Intracochlear ECochG along the array. Top rows: measurements in the two different subjects, first and second row representing subjects ID-1 and ID-2 respectively. The recording electrode number on the x-axis varies from 1 (the most apical) to 15 (the most basal). Recordings were done at the odd electrode contacts only. Lowest rows: modeled CM responses (in μV) at 16 electrode positions for the C1 - MS configuration in response to low stimulus levels (20 - 60 dB SPL, third row) and high stimulus levels (70 - 100 dB SPL, fourth row). Each column shows the response to a different stimulus frequency (250-4000 Hz). Grey scale indicates stimulus level, increasing from light to dark.

Effect of cochlea and implant on the response along the array

To investigate effects of cochlear morphology and implanted electrode design, CM responses to 90 dB SPL were modeled for each cochlea-implant configuration (figure 6.8). The electrode location where the maximum response was recorded was slightly different for each configuration. In response to 250 or 500 Hz stimuli, a second peak was recorded basally in all configurations. The exact location and size of this second peak however differed per configuration. In response to 1000 Hz only the response in the C2-1J configuration showed a double peak. The 4kHz CM amplitudes along the array exhibit a jagged response in configurations B, C and D.

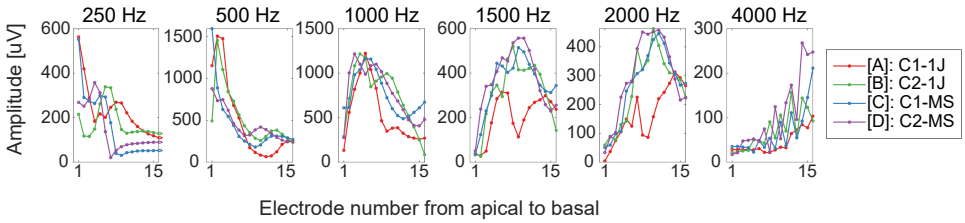

Figure 6.8. Modeled CM responses for the different cochlea-implant configurations, in response to a stimulus of 90 dB SPL. Each graph shows the response to a different stimulus frequency (250-4000 Hz). Each color shows a different configuration; [A]: cochlea 1, 1J in red; [B]: cochlea 2, 1J in green; [C]: cochlea 1, MS in blue; [D]: cochlea 2, MS in purple. X-axis denotes the electrode location.

6

Effect of hair cell type and degeneration on the response along the array

ECochG responses from IHCs and OHCs were simulated separately to evaluate how hair cell type affected the intracochlear pattern. Simulations of how different types of hair cells contributed to the intracochlear CM response are shown in figure 6.9. The peak of the response originating from IHCs was narrower than the response originating from OHCs. Response amplitudes increased faster with stimulus levels for IHCs than for OHCs. The OHC responses showed double peaks, especially in response to higher stimulus levels. This was also seen in the recordings from subject ID-1 in figure 6.7.

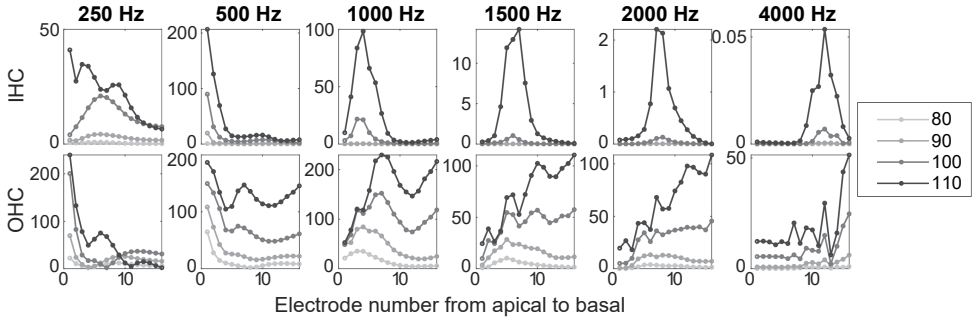

Figure 6.9. Effect of hair cell type; Simulated intracochlear CM responses along the electrode array originating solely from IHCs (top row) and originating solely from OHCs (lower row). Simulations were done with the intact cochlea. Hair cell survival rate was set at 100% and c-factors at 1. Simulations show responses to stimulus levels of 80- to 110- dB SPL and stimulus frequencies of 250- to 4000 Hz.

To investigate the effect of hair cell damage on the intracochlear CM, responses are simulated for four different degrees of hair cell degeneration. Results are shown in figure 6.10. CM responses were very similar when hair cell damage was equally distributed (hearing loss degrees HL-A and HL-B). Sloping hair cell damage, as in HL-C, resulted in

smaller response amplitudes to high stimulus frequencies on the basal electrodes, compared to HL-B. A basal dead region (HL-D), resulted in minimal activation at the 5 most basal electrode contacts (electrode number 11 – 15) in response to stimulus frequencies of 1 kHz and higher.

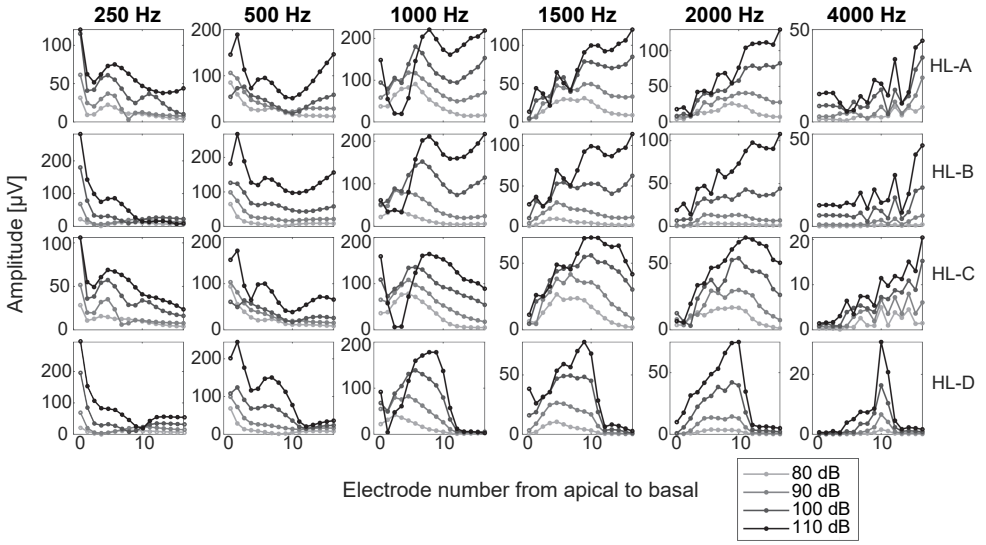

Figure 6.10. Effect of hair cell survival; Simulated intracochlear CM responses along the electrode array in cochleae with different configurations of hair cell survival. The different hair cell configurations are referred to as HL-A, HL-B, HL-C and HL-D. Simulations show responses to stimulus levels of 80- to 110- dB SPL and stimulus frequencies of 250- to 4000 Hz.

4 DISCUSSION

A model was developed that replicated characteristics seen in intracochlear ECochG recordings in the temporal, spectral and spatial domain. Simulations with different degrees and size of hearing loss yielded similar results as recordings from two different subjects. 3D volume conduction simulations showed that the intracochlear ECochG is a local measure of activation. This local sensitivity was reflected in the steep fall-off of impedances with distance along the basilar membrane (figure 6.4). In line with the theory of place-coding, and the level-dependency of hair cell activity, increasing stimulus level resulted in wider tuning curves. The peaks shifted basally with increasing stimulus frequency. The exact location on the array of the peak CM amplitude depended on cochlear morphology and implant type. Double peaks were seen in response to the highest stimulus levels. These double peaks could be either attributed to cross-turn sensitivity or wide tuning of the hair cells. The width of the tuning was different in both subjects. Simulations showed that different tuning width could results from different stimulus levels, morphologies and

degrees and types of hearing loss. Differences in hearing loss could explain differences between the recordings from the two subjects in terms of CM onset responses, higher harmonics, and the width of the tuning curve. Concluding, the model reproduced intracochlear hair cell responses recorded from CI-subjects and can be used to investigate effects of individual differences.

Cochlear morphology and electrode design

While the impedance curves in Figure 6.4 are primarily determined by the distance between the recording electrode contacts and the individual hair cells, they are also affected by other geometric factors such as the relative orientations of the recording contacts and hair cells, as well as the size and positioning of the electrode array's silicon carrier. In the models of the 1J array, the silicon carrier can be pressed up close to the basilar membrane at various points (e.g. see inset of figure 6.2A), which partially insulates the recording contacts from the current generated by the hair cells. This results in a more irregularly shaped set of impedance profiles for the 1J compared to the MS arrays (compare the peak impedance values in figures 6.4A&B to 6.4C&D), since the MS array's mid-scalar positioning offers a clearer and more consistent current pathway from hair cell to electrode through the scala tympani. Counter-intuitively, this also leads to lower peak values in the impedance curves for the 1J at certain insertion angles, despite the 1J being positioned closer to the basilar membrane than the MS (e.g. compare peak values between the 1J and MS at around 180° in figures 6.4A and 6.4C).

The jagged responses in the CM recordings along the array in response to 4 kHz originate from the OHC responses (figure 6.9), which had a much wider activation than IHCs. The OHC responses to 4 kHz showed a relatively quick change in phase along the basilar membrane, and as a consequence, the way these responses add to a CM-signal on an individual electrode is highly influenced by the exact phases of the OHC-responses in its neighborhood.

Hearing loss and the intracochlear ECochG

Different degrees of hair cell degeneration yielded responses that mimicked characteristics of recorded responses, in the temporal and spectral domain (cf. figures 6.5 and 6.6) and in the spatial domain (cf. figures 6.7, 6.9 and 6.10). In the summed response recorded from subject ID-1 no AC component was above noise floor (figure 6.5). Simulations showed lower AC components in the summed response when only IHCs were modeled or in HL-B. Recorded difference responses in subject ID-1 (figure 6.5) showed a clear CM, but no onset response and no harmonics. In the simulations this is seen when only IHCs or only OHCs were modeled, or when low c-factors were applied (0.1 or less in the models HL-B and HL-D). Recordings from subject ID-1 showed narrow tuning curves, which was replicated in the model by removing OHCs, but retaining all the IHCs. The simulations therefore suggest that subject ID-1 suffered from (near-)complete OHC loss or large functional damage to the OHCs. In line with this observation, subject ID-1 had a flat audiogram and relatively good audiometric thresholds.

In subject ID-2 the second harmonic was present in the summed response, which was seen in most simulations except in the simulation HL-B. In the difference response the CM was large and a prominent onset response was observed. Higher harmonics were clearly visible in the spectral domain. Onset responses and higher harmonics were seen in the HL-A and HL-C simulations or in a healthy cochlea. These simulated conditions all had high c-factors, up to 1 in the apical regions. The onset response was not seen when only IHCs or OHCs were modeled. This suggests that it is an interaction effect caused by phase differences between the IHCs and the OHCs at onset. The width of the responses along the array in subject ID-2 is most similar to the widths in HL-A and HL-B, where hair cell degeneration was equally distributed along the basilar membrane. The simulations thus suggest that subject ID-2 has good functioning IHCs and OHCs, but that their numbers are reduced equally throughout the cochlea.

IHCs and OHCs contribute differently to the intracochlear ECochG

Evaluating the separate IHC and OHC contributions (figure 6.9) showed that the intracochlear ECochG CM response is dominated by OHCs, especially in response to high stimulus frequencies. OHC domination of the ECochG response is consistent with animal experiments (Dallos, 1986, 1985, 1983; Dallos et al., 1972; Dallos and Cheatham, 1976; Davis et al., 1958; Russell et al., 1986). Modeled electrical impedances were similar between IHCs and OHCs, and hence impedance differences cannot explain the difference. OHC voltages as produced by the hair cell model are generally four times smaller than the IHC voltages. OHCs are about three times larger in number than IHCs. Both those facts combined would expect equal total contributions from IHCs and OHCs. A possible explanation for the larger OHC contribution is a difference in low-pass-filtering membrane properties between IHCs and OHCs. The low-pass filtering cut-off frequencies for the IHCs are generally lower than those of the OHCs(Johnson et al., 2011), which results in a relative insensitivity of the ECochG to the IHC AC voltages.

Animal studies correlating post-mortem histological counting of the hair cells to audiometric thresholds have shown that hair cell degeneration generally starts in the base and then proceeds to the apex. Laterally positioned hair cells are more vulnerable than those medially positioned. Hence, it is believed that degeneration generally progresses from base to apex, and affects lateral OHCs first and the medially positioned IHCs last (Dallos et al., 1972; Eric Lupo et al., 2011; Stebbins et al., 1979; Van Ruijven et al., 2005, 2004). Synaptic or retro-cochlear pathologies might cause hearing loss regardless of the status of hair cells in the cochlea (Hill et al., 2016).

Limitations of the model and future research

A challenge in modeling hair cell membrane behavior is the relatively sparse animal data available. In the present study the dependency of conductance parameters on the CF was determined from a few different data points only (Johnson et al., 2011). A wider range of data showing how the hair cell conductance depends on CF is desirable. Another limitation is the unusually large IHC responses to stimulus levels above 80 dB SPL compared to animal data (see appendix). Lastly, from the auditory peripheral model, only responses to hair cells with a CF higher than 125 Hz could be obtained, although hair cells with lower CFs might also contribute to the ECochG response. The current study focused on the CM response. Instead, the SP could perhaps also be used as a diagnostic marker of electrode position (Helmstaedter et al., 2018). This could be further evaluated with the here presented model. The model can also be extended with neural firing to simulate CAP and ANN responses, to disentangle these from hair cell responses. The model of the auditory periphery does include a nerve fiber model, which could simulate spiking, and hence, CAP and ANN responses could be modeled as well. For this purpose, single fiber contributions to the ECochG would have to be estimated first. The model developed here could also be used to predict extracochlear recordings, close to the round window. Effects of often used stimulation patterns, such as chirps or tone bursts, or newly suggested patterns such as partially noise-masked tones (Chertoff et al., 2012), could be modeled. By using the 3D model for this, also complex projections from the hair cells to the extracochlear electrode are taken into account.

APPENDIX

Comparison of simulated and recorded membrane voltages

Previously, it was shown that the relative dependency of IHC voltage on stimulus level and frequency is correctly predicted by the hair cell model (Zhang et al., 2001). In addition, this appendix shows qualitative similarities and discrepancies between simulated and previously recorded IHC and OHC voltages.

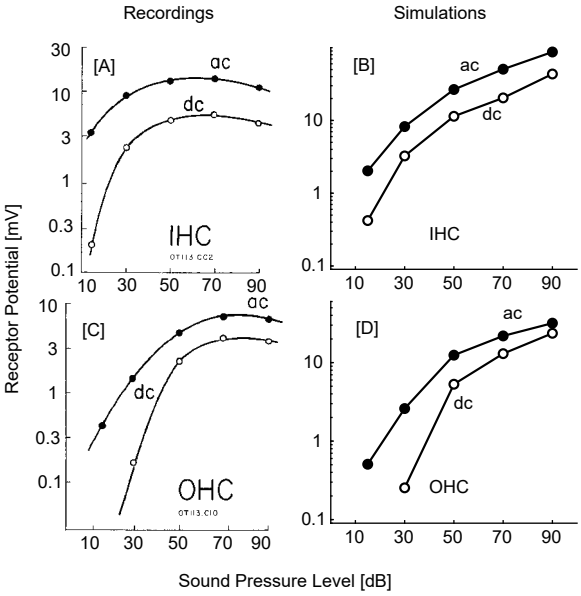

Figure 6.11. Measured [A&C] and simulated [B&D] input-output functions of intracellular responses to acoustic stimuli presented at 800 Hz. AC and DC responses are plotted for both IHCs [A&B] and OHCs [C&D]. AC responses were defined as the peak value of the fundamental component derived from the tone burst responses, while DC responses were defined as the mean of the response in the second half of the stimulation in both model and physiological data. The physiological recordings were obtained from Dallos (1985) [reprinted with permission].

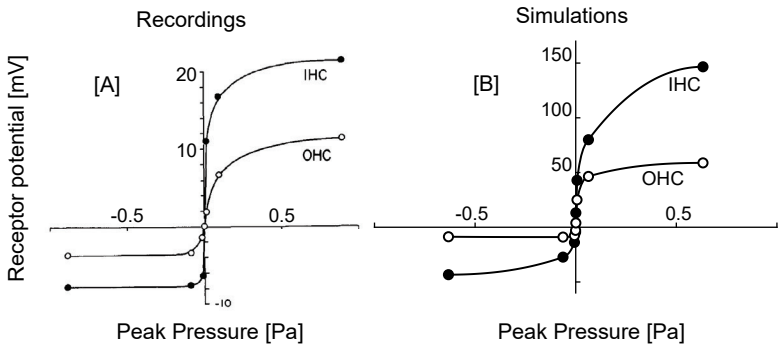

Figure 6.12. recorded [A] and simulated [B] max receptor potentials showing peak AC receptor potentials as a function of peak sound level, in response to stimulation at characteristic frequency (800Hz). The fit for simulations was done piecewise polynomial with constraints to the endpoints, the fit for the recordings is unknown. The physiological recordings were obtained from Dallos (1986) [reprinted with permission].

Figure 6.11 shows that the ratio between AC and DC response amplitudes is correctly simulated. The amplitudes of the simulated and recorded AC and DC components in both IHCs and OHCs increase with sound pressure level, but saturation is stronger in the recordings than in simulations. Figure 6.12 shows that the model successfully reproduces nonlinear behavior in both IHCs and OHCs. In both simulations, the absolute levels were comparable in response to the low stimulus levels, but up to a factor four larger in the simulations in response to high stimulus levels. An explanation for this is that the absolute response amplitudes are dependent on placement of the reference electrode. Overall, qualitative behavior of potentials of both types of hair cells in response to different stimulus levels is well described by the model.